

# Small-angle neutron scattering from typical synthetic and biopolymer solutions

Ferenc Horkay · Boualem Hammouda

Received: 17 December 2007 / Revised: 28 January 2008 / Accepted: 31 January 2008 / Published online: 4 March 2008  
© Springer-Verlag 2008

**Abstract** Small-angle neutron scattering (SANS) has been used to investigate the solution properties of four model polymers, two poly-amino acids [poly(lysine) and poly(proline)], and two water-soluble synthetic polymers [poly(acrylic acid) and poly(ethylene oxide)]. In each case, one of the two polymers is charged, while the other is neutral. SANS measurements were made in the semi-dilute concentration regime in two different solvents [*d*-water and *d*-ethylene glycol]. The scattering signals were decomposed into low-*Q* clustering and high-*Q* solvation contributions. The temperature dependence of the scattering parameters was determined for poly(lysine) and poly(ethylene oxide) solutions over the temperature range of 13 to 82 °C. Analysis of the SANS spectra revealed that with increasing temperature, the solvation intensity increased in both solvents, while the clustering intensity increased in *d*-water and decreased in *d*-ethylene glycol. Significant differences were observed between the SANS spectra of charged and neutral polymer solutions. However, biopolymers and synthetic polymers exhibited qualitatively similar behavior.

**Keywords** Small-angle neutron scattering · Polymer solution · Solvation · Clustering · Hydrophilic/hydrophobic interaction

## Introduction

Current trends in the field of biomedical sciences indicate the need for techniques that provide structural and thermodynamic information of complex systems at different levels of hierarchical organization. Small-angle scattering methods allow us to investigate biopolymer molecules in their natural environment and to correlate the changes in the environmental conditions (e.g., temperature, solvent quality, ionic strength) with physical properties such as molecular conformation and osmotic compressibility [1, 2]. In recent years, small-angle neutron scattering (SANS) and small-angle X-ray scattering (SAXS) have become fundamental tools in the study of polymers on the nanometer length scale. Unlike other methods, SANS and SAXS provide useful information about the properties of partially or completely disordered systems such as polymer solutions and gels.

The value of these techniques in polymer and biological sciences becomes clear when the length scales are considered: bond lengths are of the order of 1 Å, the size of a flexible polymer molecule in solution is between 10 and 1,000 Å, the persistence length of a double-stranded DNA molecule is about 500 Å, while the diameter of viruses varies from a few hundred to several thousand Ångströms.

In typical physiological systems, such as cells and tissues, macromolecules occupy a considerable fraction (up to 40–50%) of the total volume. The high overall concentration is due to the large number of different macromolecular species in the media. Usually, these systems are called crowded rather than concentrated because the concentration of the

---

F. Horkay (✉)

National Institutes of Health, NICHD,  
Laboratory of Integrative and Medical Biophysics,  
13 South Drive,  
Bethesda, MD 20892-5772, USA  
e-mail: horkay@helix.nih.gov

B. Hammouda

National Institute of Standards and Technology,  
Center for Neutron Research,  
100 Bureau Drive,  
Gaithersburg, MD 20899-6102, USA

individual polymeric components is relatively low. In a crowded environment motion of large molecules is hindered by mobile and immobile barriers. Molecular crowding may also influence molecular conformation and interaction between macromolecules.

SANS probes the structure at the nanometer scale and simultaneously provides information on the thermodynamic properties. The mechanism by which the incident neutrons interact with matter is fundamentally different from other scattering methods [2–5]. In the case of light and X-rays, the scattering cross-section of the atoms increases proportionally with the number of electrons, whereas the neutron scattering lengths vary erratically from one element to another. Specific deuteration makes it possible to highlight selected parts of the polymer molecules. In complex systems, information about the distribution of the components can be obtained by mixing deuterated and protonated solvents, i.e., by varying the scattering length density of the solution [6, 7]. Another important advantage of neutrons compared to X-rays is that their interaction with the nuclei is relatively weak, making them highly penetrating and non-destructive. Therefore, neutrons can be used to study the bulk properties of sensitive samples, such as biological materials.

Over the past decades, the majority of SANS investigations have focused on synthetic polymers with a few biological (mostly protein conformation) studies. Our ongoing efforts described in this paper reflect the change in trend from mostly synthetic polymer research to biopolymer research. To bridge the gap between the synthetic polymer community and the biology community, we focus on relatively simple biopolymers, namely poly-amino acids.

We studied a set of four model polymers (two water-soluble synthetic polymers and two poly-amino acids) using SANS. The synthetic polymers were poly(acrylic acid), which is charged and poly(ethylene oxide), which is neutral. The two investigated poly-amino acids were poly(lysine), which is polar and charged (dissolves easily in water), and poly(proline), which is non-polar and uncharged (poorly soluble in water). In aqueous environment, poly(lysine) yields a polyelectrolyte solution, while poly(proline) behaves like a neutral polymer.

The aim of this paper was to identify common features in the structure and thermodynamic behavior of synthetic and biopolymer solutions. We demonstrate that SANS is particularly well suited to study intermolecular interactions between polymers and solvent molecules, such as hydration and solvation, as well as self-assembly and large-scale organization on which biological function often relies. We focus on the semi-dilute concentration regime in which the polymer coils overlap with each other, thus mimicking the molecularly crowded environment. The results are presented in terms of simple concepts and ideas with minimum

mathematics. We hope that conveying basic ideas and fundamentals in a descriptive manner may help bridge the gap between diverse scientific communities (colloid and polymer scientists, biophysicists, biologists, etc.) involved in the research on biopolymers.

The paper is organized as follows. We begin by a brief description of the basic principles of small angle scattering measurements with particular emphasis on the thermodynamic information that can be derived from SANS studies on polymers. SANS results obtained for solutions of four different polymers in D<sub>2</sub>O are then presented. The scattering spectra are analyzed by decomposing the SANS signal into clustering (low-Q region) and solvation (high-Q region) contributions. A comparison is made between the scattering response of charged polymers in salt-free solutions and in the presence of added salt (0.1 M NaCl in D<sub>2</sub>O). Finally, SANS results obtained for the same four polymers in deuterated ethylene glycol are presented and compared with those measured in D<sub>2</sub>O.

### Physical principles of SANS measurements

SANS provides information about the form (size and shape) and spatial arrangement of the structural elements in solution as well as their inter-particle interactions over the so-called mesoscopic scale covering the length scale range from 10 to 1,000 Å [8–9].

In a SANS experiment, a monochromated and collimated beam of neutrons is incident upon the sample, and the intensity of scattered radiation is measured as a function of the scattering angle. The fundamental relationship governing the experiment is given by the scattering amplitude

$$f(Q) = \int_V d^3r \exp(i\mathbf{Q}\cdot\mathbf{r})n(r) \quad (1)$$

where  $V$  is the sample volume,  $n(r)$  is the scattering density, and  $Q$  is the scattering variable. The scattering intensity is defined by the average of the square of  $f(Q)$ . The integral in Eq. 1 extends over the whole volume of the sample. The scattering vector is given by the formula

$$Q = \frac{4\pi}{\lambda} \sin\left(\frac{\theta}{2}\right) \quad (2)$$

where  $\lambda$  is the neutron wavelength and  $\theta$  is the scattering angle. The quantities  $Q$  and  $r$  in Eq. 1 are reciprocally related (Fourier transform pair) and, as a consequence, larger structures are probed at lower values of  $Q$ , or (according to Eq. 2) at smaller angles for fixed wavelength.

The SANS results are complementary to other high and low-resolution techniques (e.g., X-ray diffraction, electron microscopy, nuclear magnetic resonance, light scattering),

thus making it possible to construct detailed structural models and to improve and reconcile concurrent theories.

### Thermodynamic considerations

Phase transitions are common phenomena in polymer solutions [10]. The tendency of polymer/solvent systems to demix is due to the large difference in the size of polymer and solvent molecules. This difference also causes the phase diagram to become highly asymmetric. Figure 1 shows the case of a binary polymer solution exhibiting a lower critical solution temperature (LCST, phase separation occurs upon heating), which is typical for water-soluble polymer systems. The opposite case, partial immiscibility upon cooling, also occurs frequently and is described by an upper critical solution temperature (UCST). For certain systems, one cannot reach phase separation upon cooling because the solvent solidifies. Similarly, the solvent may boil upon heating (at atmospheric pressure) before demixing takes place.

In the upper part of Fig. 1, the solid curve, often called the coexistence curve, represents the equilibrium condition. Liquid mixtures with compositions inside this curve separate into two phases of compositions  $\varphi_1$  and  $\varphi_2$ . The two-phase region is further divided into two subregions separated by the dashed curve (spinodal line). A single phase between the solid (binodal) and dashed lines is metastable to small concentration fluctuations but unstable to large concentration fluctuations. There is a minimum temperature “critical point” at which the binodal and spinodal lines coincide. The lower part of the figure represents the

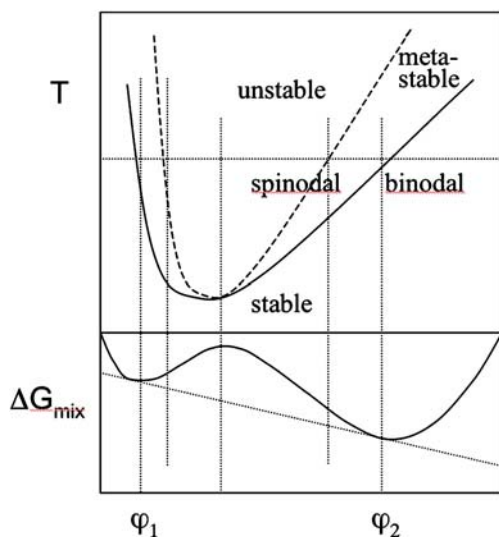


**Fig. 1** Schematic phase diagram of a binary polymer solution exhibiting lower critical solution temperature (LCST). The lower part of the figure shows the Gibbs free energy of mixing as a function of composition

variation of the Gibbs free energy as a function of composition. According to the second law of thermodynamics for systems at equilibrium at a given temperature  $T$  and pressure  $P$ , the coexisting phases must have the lowest Gibbs free energy  $\Delta G_{\text{mix}}$  (corresponding in composition to the two minima) [11–12].

Three terms contribute to the Gibbs free energy of mixing: the internal energy of mixing, which accounts for intermolecular interactions, the entropy of mixing, and the volume of mixing

$$\Delta G_{\text{mix}} = \Delta E_{\text{mix}} - T\Delta S_{\text{mix}} + P\Delta V_{\text{mix}} \quad (3)$$

In low-molecular-weight fluids, immiscibility (demixing) can be explained by weak repulsive interactions. The entropic contribution, which is always positive, becomes more significant as the temperature increases and drives the system to mix at a UCST.

The situation is more complicated for polymers. The solvent is much more compressible than the polymer, and the increasing difference in compressibility with increasing temperature leads to a negative volume of mixing. For polymers, the entropic contribution is relatively small, as macromolecules can assume fewer configurations than small molecules, and the difference in the compressibility of the polymer and solvent mixture governs the phase separation. The LCST behavior, observed in many polymer/solvent systems, is the consequence of such compressibility effects.

At the molecular level, phase separation is accompanied by large concentration fluctuations. These fluctuations have a certain characteristic length scale, referred to as the correlation length  $L$ . Far from the critical point (in the single-phase region), the correlation length is typically comparable to the size of the components in solution. As phase separation is approached,  $L$  increases and diverges at the critical point.

Physical quantities relevant to the critical behavior of polymer solutions are experimentally accessible. Scattering of radiation arises from random thermal concentration fluctuations. The scattering intensity,  $I(Q)$ , which is proportional to the Fourier transform of the spatial correlation function of the concentration fluctuations, can be determined by SANS or SAXS and is given by the form

$$I(Q) = \frac{k_B T \Delta \rho^2}{K} F(x) \quad (4)$$

where  $F(x)$  is a scaling function,  $K$  is the osmotic compressibility,  $\Delta \rho^2$  is the scattering contrast factor,  $k_B$  is the Boltzmann constant, and  $T$  is the absolute temperature. For polymer solutions,  $F(x)$  can be given by the Ornstein–Zernike expression (Lorentzian function) [13]

$$F(x) = 1 / (1 + x^2) \quad (5)$$

where  $x = QL$ .

The scattering intensity and its  $Q$  dependence yield information about the thermodynamic properties of the system, such as the osmotic compressibility of the polymer solution and the correlation length of the thermal concentration fluctuations. In polymer systems, particularly in polyelectrolyte solutions, clustering often plays an important role. Large clusters do not contribute significantly to the thermodynamics of the solution but strongly modify the scattering spectrum in the low- $Q$  range. For many polyelectrolyte solutions  $I(Q)_{\text{cluster}}$  decreases rapidly with  $Q$  [ $I(Q)_{\text{cluster}} \sim Q^{-n}$ , with  $2 < n < 4$ ]. We note that the total scattering intensity observed by SANS also contains an incoherent contribution, which is independent of  $Q$ . According to our scenario, the total SANS intensity is given as a sum of three contributions

$$I(Q) = I(Q)_{\text{cluster}} + I(Q)_{\text{solvation}} + I_{\text{incoherent}} \quad (6)$$

In Eq. 6, the first term describes the scattering from large clusters, while the second term originates from the thermal concentration fluctuations and is governed by the solvation (hydration) of the polymer chains.

### Polymers and solvents

The polymers used in the present work were purchased from Sigma-Aldrich and used as received. Poly(acrylic acid) sodium salt had a narrow molecular weight distribution with  $M_w=127,500$  g/mol and  $M_n=117,000$  g/mol. The molecular weight distribution of poly(ethylene oxide) was also relatively narrow with  $M_w=41,500$  g/mol and  $M_n=36,500$  g/mol. Poly-L-lysine hydrobromide had a broader molecular weight distribution  $M_w=300,000$  g/mol and  $M_n=150,000$  g/mol. The molecular weight of poly(proline) was smaller  $M_w=40,000$  g/mol and  $M_n=30,000$  g/mol. The chemical formulas of the polymers are shown in Fig. 2.

We note that all of the SANS measurements reported in this paper were made on semi-dilute polymer solutions. In the semi-dilute concentration regime, i.e., above the overlap concentration, the individual polymer chains are indistinguishable, and the osmotic pressure of the solution no longer depends on the molecular weight of the polymer [13]. For a flexible polymer of molecular weight 40,000 g/mol in good solvent conditions, the overlap concentration is below 2%.

Solutions containing 4% (g/g) polymer were prepared at room temperature in two different solvents: *d*-water (deuterated or “heavy” water), and *d*-ethylene glycol (deuterated ethylene glycol). This polymer concentration is well beyond the overlap concentration even for the lowest molecular weight sample. *d*-Ethylene glycol (DOCD<sub>2</sub>CD<sub>2</sub>OD) contains both hydrophobic (–CD<sub>2</sub>–) and hydrophilic (–OD) groups. Two more samples were made by adding 0.1 M NaCl to the solutions of the two charged

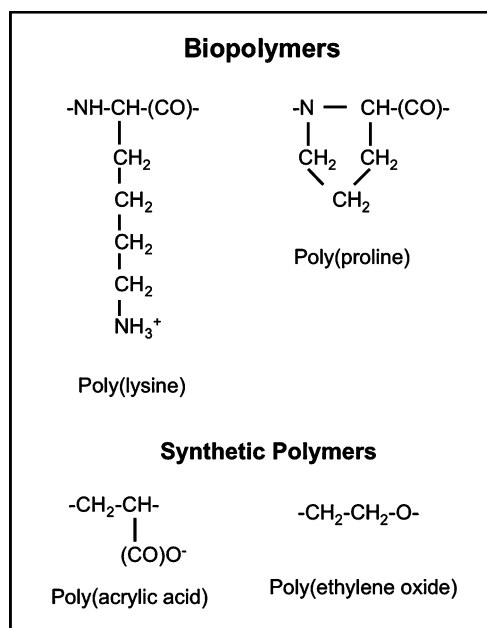


Fig. 2 Chemical formulas for the four model polymers used

polymers [poly(lysine) and poly(acrylic acid)] in D<sub>2</sub>O. The pH of the solutions was around 7. All samples were investigated by SANS at 25 °C. To obtain information on the effect of temperature on the phase diagram of poly(lysine) and poly(ethylene oxide) solutions, SANS measurements were made in both D<sub>2</sub>O and *d*-ethylene glycol at seven different temperatures: 13, 25, 37, 49, 63, 82 °C (and then after cooling down to 26 °C).

We note that poly(proline) cannot be easily dissolved in either of these solvents. The 4% poly(proline)/D<sub>2</sub>O solution exhibited slight haziness, and the 4% poly(proline)/*d*-ethylene glycol solution remained “white” even at 82 °C, indicating the presence of large inhomogeneities.

### SANS measurements

SANS measurements were made at the NIST Center for Neutron Research on the NG3 instrument using three configurations: low- $Q$ , intermediate- $Q$ , and high- $Q$ . These experimental configurations covered the  $Q$ -range  $0.0035 \text{ \AA}^{-1} < Q < 0.45 \text{ \AA}^{-1}$  corresponding to size scales from 0.18  $\mu\text{m}$  (low- $Q$ ) to 14  $\text{\AA}$  (high- $Q$ ). Standard empty cell and blocked beam corrections and data treatment methods were applied [14].

The SANS data were analyzed using a simple functional form that reproduces the main characteristic features of the scattered intensity  $I(Q)$  vs  $Q$  curves

$$I(Q) = A/Q^n + C/[1 + (|Q-Q_0|L)^m] + B \quad (7)$$

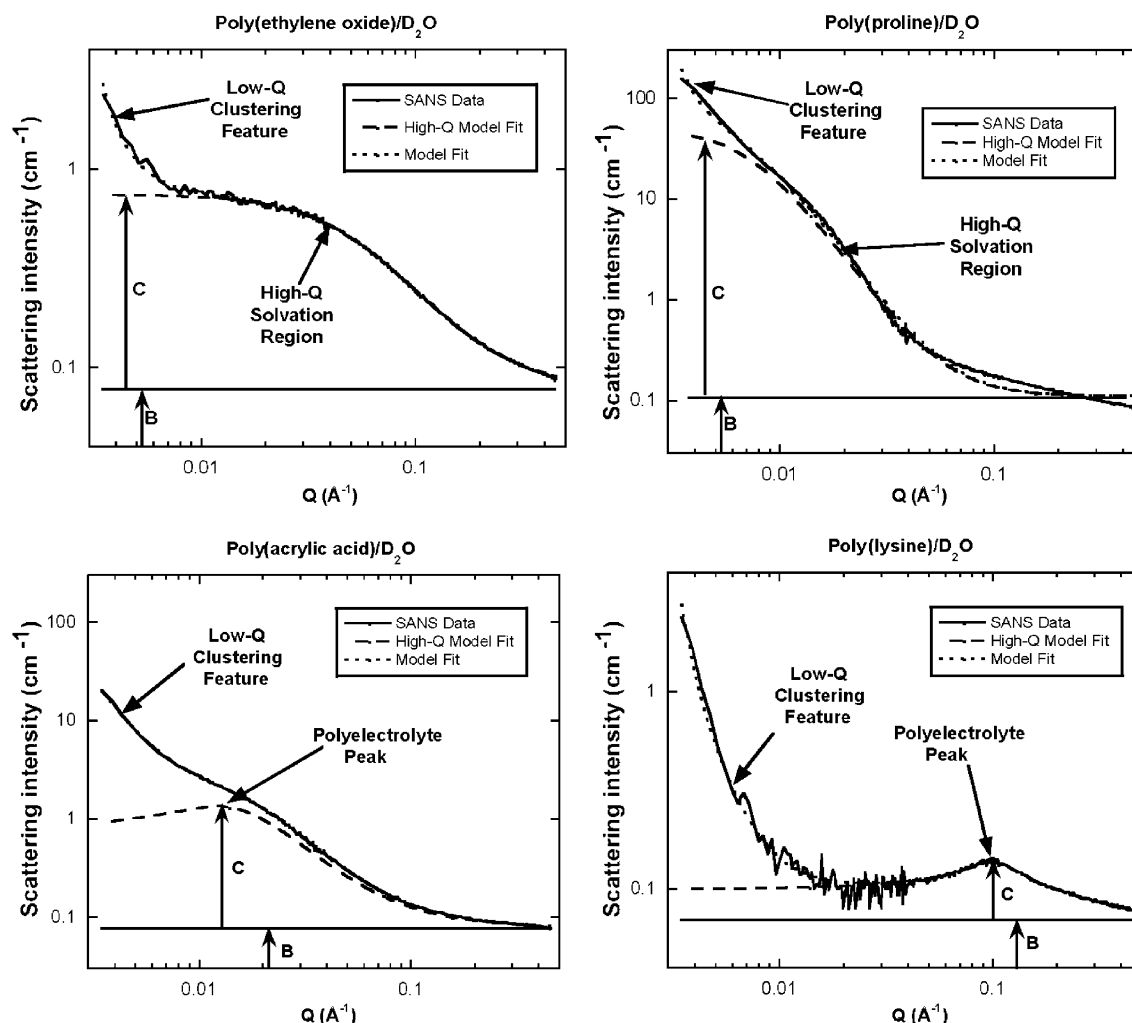


**Fig. 3** SANS data from the four polymer solutions in  $D_2O$  at 25 °C. Parameter  $C$  is called the solvation intensity, and  $B$  is the background

The basic features are the low- $Q$  clustering term  $A/Q^n$  (where  $Q=0.004 \text{ \AA}^{-1}$  was used throughout as a low- $Q$  value) and the high- $Q$  solvation term  $C/[1 + (|Q-Q_0|L)^m]$ . In Eq. 7,  $n$  and  $m$  are the clustering and solvation Porod exponents,  $L$  is a correlation length, and  $Q_0$  is the peak position (when applicable).  $Q_0$  is finite for solutions of charged polymers, and  $Q_0=0$  for neutral polymer solutions.  $B$  is a constant background mostly due to incoherent scattering.<sup>1</sup>  $A$ ,  $n$ ,  $m$ ,  $C$ ,  $L$ ,  $Q_0$ , and  $B$  are all floating parameters in the nonlinear least squares fits to the SANS data. Note that the size of the clusters is large (micron size) and cannot be completely resolved by the SANS instrument. Only its tail is observed and can be approximated by the  $A/Q^n$  term.

<sup>1</sup> We note that the conventional way of estimating the incoherent background from measurements on different  $H_2O/D_2O$  mixtures and interpolating the data to the desired concentrations yields similar results. In  $H_2O/D_2O$  mixtures, the incoherent contribution is a function of the  $H_2O$  content, as the coherent contribution for  $H_2O$  is negligible.

In Fig. 3, representative SANS spectra are displayed showing the low- $Q$  clustering part and the high- $Q$  solvation part along with the model fits to Eq. 7. The high- $Q$  part of the model fit is defined by the middle term in Eq. 7.

### Results for $D_2O$ solutions

Figure 4 shows the reduced SANS data for the four polymer solutions in  $D_2O$  at 25 °C. Each polymer solution exhibits two common features: low- $Q$  clustering and high- $Q$  solvation. The clustering part points to large (micron size) gel-like structures, and the solvation part provides information about the solvation sheath around the chains. Clustering is pervasive and is observed in most aqueous polymer solutions. The size of the clusters exceeds the resolution of the SANS experiment. Solvation is governed by the interaction between the polymer and the solvent molecules and drives the thermodynamics of phase separation. We note that in  $D_2O$  solutions, H–D exchange occurs



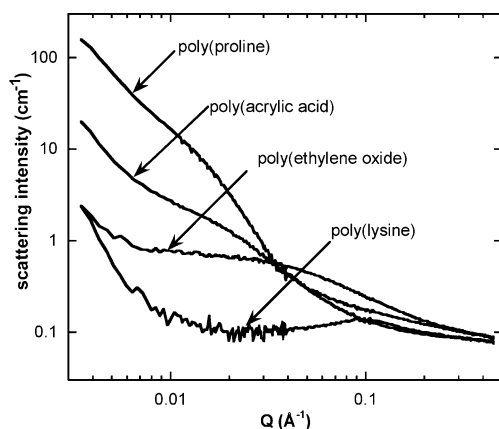


**Fig. 4** SANS scattering intensity for polymer solutions in D<sub>2</sub>O measured at 25 °C. The two charged polymers [poly(lysine) and poly(acrylic acid)] show polyelectrolyte solution behavior as evidenced by the polyelectrolyte peak. The polyelectrolyte peak in the poly(acrylic acid) solution has merged with the low-Q clustering feature. Both uncharged polymers [poly(proline) and poly(ethylene oxide)] display neutral polymer solution behavior. We note that the precision of the data scales with the height of the jagged drawing lines

in polymers containing labile protons (NH and OH groups). Although, this process does not influence the overall shape of the scattering curve it modifies the scattering contrast ( $\Delta\rho^2$  in Eq. 4).

Polymer solvation is characterized by either a polyelectrolyte peak at finite  $Q_0$  (charged molecules) or a forward scattering peak (neutral polymers) for the high-Q signal. The solutions of both charged polymers [poly(lysine) and poly(acrylic acid)] display a correlation peak typical of polyelectrolyte systems. In the poly(lysine) solution, the peak occurs at  $Q_0 \approx 0.1 \text{ \AA}^{-1}$ , corresponding to an average distance of  $d_0 = 2\pi/Q_0 = 63 \text{ \AA}$  between the charged domains. In the poly(acrylic acid) solution, the polyelectrolyte peak is not well resolved from the low-Q clustering feature. The two neutral polymers [poly(proline) and poly(ethylene oxide)] are characterized by high-Q signals peaked in the forward scattering direction ( $Q_0=0$ ).

We also made SANS measurements on the solutions of the two charged polymers in D<sub>2</sub>O in the presence of 0.1 M NaCl (Fig. 5). Addition of salt screens the charges, therefore making the charged domains larger [14]. This shifts the polyelectrolyte peak position towards lower values of  $Q$ , and the SANS spectrum of the polyelectrolyte solution becomes similar to that of a neutral polymer solution. In 0.1 M NaCl solution, the position of the poly(lysine) peak moved from  $Q_0=0.1 \text{ \AA}^{-1}$  (without salt) to  $Q_0=0.047 \text{ \AA}^{-1}$  (in 0.1 M NaCl), indicating that the size of the charged domains was roughly doubled. In the case of poly(acrylic acid), the polyelectrolyte peak (around  $Q_0=0.02 \text{ \AA}^{-1}$ ) has completely merged with the clustering feature.

In what follows, we focus on the temperature dependence of the SANS spectra of the solutions of a charged and an uncharged polymer. To reveal the effect of temperature on

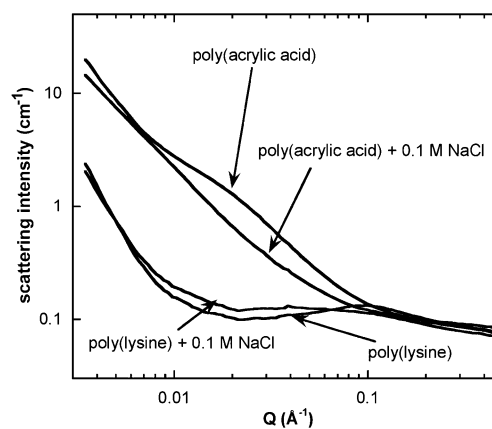


**Fig. 5** SANS scattering intensity for 4% poly(lysine) and 4% poly(acrylic acid) in D<sub>2</sub>O at 25 °C without and with added salt (0.1 M NaCl). In the presence of added salt, the polyelectrolyte peak moves to lower  $Q$  and the peak intensity decreases. In poly(lysine) solution, the polyelectrolyte peak is well resolved, whereas in poly(acrylic acid) solution, the peak has merged with the low-Q clustering feature

the thermodynamic properties, we made SANS measurements on the poly(ethylene oxide) and poly(lysine) solutions over the temperature range of 13 to 82 °C. These two polymers are characterized by the best SANS data sets. In the case of the poly(acrylic acid), the SANS spectra cannot be easily analyzed because the low-Q clustering and the high-Q solvation peaks strongly overlap. The poor solubility of poly(proline) renders this polymer a less favorable candidate for further studies.

#### Effect of temperature on the SANS spectra in D<sub>2</sub>O solutions

Figure 6 illustrates the temperature dependence of the SANS response of a 4% poly(ethylene oxide) solution in D<sub>2</sub>O measured at six different temperatures. The intensity is seen to increase with temperature, characterizing an LCST phase behavior.

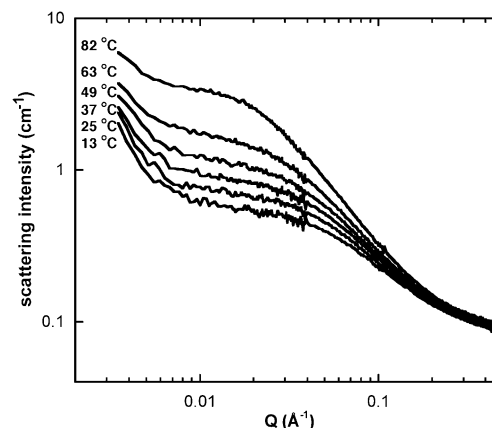


**Fig. 6** Variation of the SANS spectra with temperature for 4% poly(ethylene oxide) solution in D<sub>2</sub>O

**Table 1** Results of the nonlinear least squares fits to the SANS spectra of 4% poly(ethylene oxide) and poly(lysine) solutions in D<sub>2</sub>O (without added salt)

Polymer	13 °C	25 °C	37 °C	49 °C	63 °C	82 °C	26 °C
Clustering intensity $A/Q^n$ (cm <sup>-1</sup> ) <sup>a</sup>							
Poly(lysine)	0.63	0.65	0.59	0.67	0.68	0.81	0.82
Poly(ethylene oxide)	0.44	0.53	0.61	0.73	0.77	0.83	1.06
Solvation intensity, $C$ (cm <sup>-1</sup> )							
Poly(lysine)	0.070	0.073	0.074	0.075	0.073	0.077	0.071
Poly(ethylene oxide)	0.51	0.67	0.85	1.16	1.76	3.96	0.75
Correlation length, $L$ (Å)							
Poly(lysine)	14.97	14.56	15.31	15.28	16.38	15.85	15.53
Poly(ethylene oxide)	15.57	17.76	19.80	23.19	28.32	40.40	20.49
Porod exponent, $m$							
Poly(lysine)	1.19	1.12	1.22	1.20	1.24	1.20	1.24
Poly(ethylene oxide)	1.93	1.93	1.94	1.92	1.93	1.98	1.80
Peak position, $Q_0$ (Å <sup>-1</sup> )							
Poly(lysine)	0.100	0.099	0.098	0.098	0.095	0.094	0.098

Relative statistical errors are between 2% (low-Q features) and 4% (high-Q features) and correspond to one standard deviation.

<sup>a</sup>We used  $Q=0.004$  Å<sup>-1</sup> in the calculation of the clustering intensity.

The values obtained for all relevant parameters ( $A/Q^n$ ,  $C$ ,  $L$ ,  $m$ , and  $Q_0$ ) from the nonlinear least squares fits of Eq. 7 to the SANS spectra of both poly(ethylene oxide) and poly(lysine) solutions are summarized in Table 1.

The Porod exponent  $m=5/3$  describes the behavior of a polymer coil in a good solvent (monomer-solvent interaction is more favorable than monomer-monomer interaction), while  $m=2$  corresponds to a Gaussian coil (monomer-solvent and monomer-monomer interactions are equal in strength) [9]. These concepts apply to neutral polymer solutions. For poly(ethylene oxide)/D<sub>2</sub>O solutions,  $1.92 < m < 1.98$ , indicating that the system is near to the theta solvent condition. The values of  $m$  for poly(lysine) are significantly lower because no Porod region is distinguishable (a polyelectrolyte peak is observed instead).

In semi-dilute polymer solutions, the correlation length  $L$  is defined as the average distance between neighboring entanglement points [13].  $L$  increases with the increase of temperature in both solutions; however, the change is much more pronounced in the poly(ethylene oxide)/D<sub>2</sub>O system.

SANS probes both density fluctuations (clustering term) and composition fluctuations (solvation term). An increase in the solvation intensity (parameter  $C$ ) is an indication of the onset of phase separation. Most water-soluble polymer solutions phase separate upon heating and are characterized by an LCST. For the polymer solutions investigated in this work, the LCST lies outside of the measured temperature range. However, knowledge of the temperature dependence of  $C$  in the early stage of spinodal decomposition allows us to predict whether the polymer solution phase separates upon heating (LCST) or upon cooling (UCST). The data in Table 1 show that for both solutions,  $C$  increases with increasing temperature, which is consistent with the LCST

phase behavior. Figure 7 shows an estimate of the spinodal temperature for the poly(ethylene oxide) solution using a plot of  $1/C$  vs  $1/T$  ( $T$  is the absolute temperature). The intercept at  $1/C=0$  yields the spinodal temperature  $T_s=92$  °C. This value is in reasonable agreement with results reported in the literature [15]. (We note that for polyelectrolyte solutions, this simple linear relationship is no longer valid [16]).

The occurrence of LCST indicates that hydrogen bonds play an important role in these solutions [17–18]. At the molecular level, the phase transition is a change from hydrated random coil to hydrophobic globule. Below the LCST, the polymer is soluble due to hydrogen bonds. As the temperature rises and approaches the transition temperature, the onset of phase separation is a weakening of the hydrogen bonds formed between water molecules and the OH, NH, or C=O groups of the polymers. At elevated

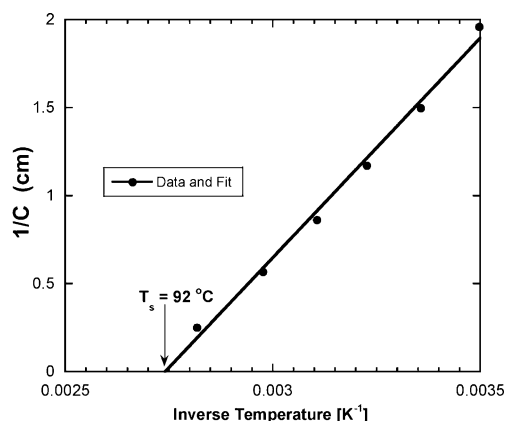


**Fig. 7** Plot of  $1/C$  vs  $1/T$  where  $C$  is the solvation intensity parameter and  $T$  is the absolute temperature for a poly(ethylene oxide) solution. The intercept at  $1/C=0$  yields the spinodal temperature

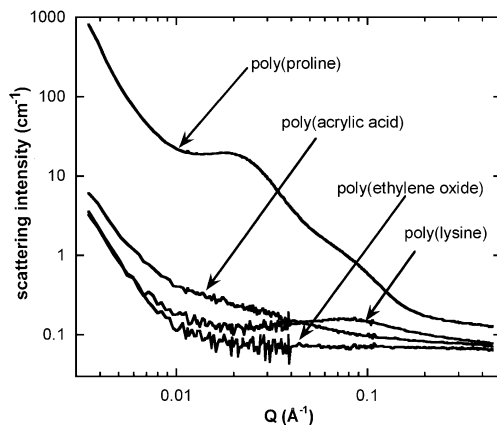


**Fig. 8** SANS scattering intensity for the four polymer solutions in *d*-ethylene glycol measured at 25 °C

temperatures, the thermal energy exceeds the hydrogen-bond energy, thereby breaking hydrogen bonds and freeing water molecules. Water progressively becomes a poor solvent as hydrogen bonds break, and hydrophobic inter-

actions between adjacent groups increase. The polymer starts to self-aggregate, followed by chain collapse into a hydrophobic globule. Consequently, polymer–polymer interactions are responsible for the aggregation and the subsequent precipitation of the polymer. Precipitation is an endothermic transition governed by a decrease of entropy.

### Results for *d*-ethylene glycol solutions

Figure 8 shows the reduced SANS data for the solutions of the four polymers in *d*-ethylene glycol at 25 °C. Although the scattering curves exhibit common features in *d*-ethylene glycol and D<sub>2</sub>O, distinct differences are detectable at both low and high values of  $Q$ .

For poly(ethylene oxide), the SANS intensity in *d*-ethylene glycol is smaller than in D<sub>2</sub>O and the shoulder at  $Q \approx 0.04$  is absent. This difference indicates that *d*-ethylene glycol is a better solvent for this polymer than D<sub>2</sub>O,

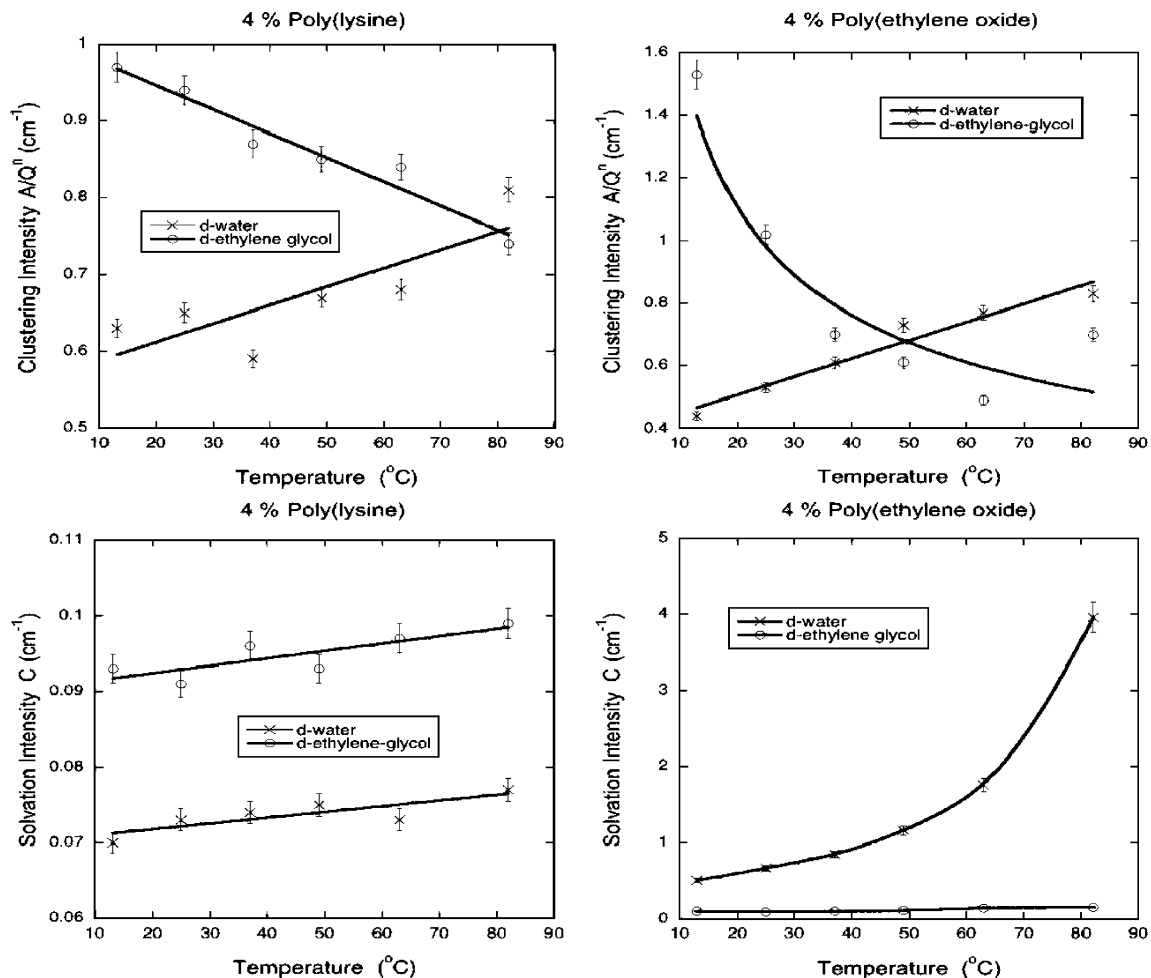


**Fig. 9** Variation of the clustering intensity (parameter  $A/Q^n$ ) and solvation intensity (parameter  $C$ ) with increasing temperature for poly(lysine) and poly(ethylene oxide) solutions in D<sub>2</sub>O and in *d*-ethylene glycol (4% mass fraction in each case). The trends are opposite for

clustering but similar for solvation. Statistical errors were obtained from the nonlinear least-squares fits and correspond to one standard deviation



probably due to the similar chemical structure of the ethylene oxide monomer and the ethylene glycol molecule. It should be noted that the scattering intensity is sensitive to changes not only in the concentration fluctuations but also in the neutron scattering contrast ( $\Delta\rho^2$  in Eq. 4). However, in the present system, the observed difference cannot be attributed solely to changes in  $\Delta\rho^2$  because the ratio of the solvation intensities in the two solvents ( $C_{D_2O}/C_{d-eg} \approx 6.67$  at 25 °C) is almost three times greater than that of the scattering contrast factors  $\left[ (\rho_{PEO} - \rho_{D_2O})^2 / (\rho_{PEO} - \rho_{d-eg})^2 = 2.24 \right]$ , where  $\rho_{PEO}$ ,  $\rho_{D_2O}$ , and  $\rho_{d-eg}$  are the scattering length densities for PEO,  $D_2O$ , and  $d$ -ethylene glycol, respectively]. In the poly-acrylic acid solution, the polyelectrolyte peak strongly overlaps with the clustering feature and cannot be resolved. The scattering spectrum of poly(lysine) in  $d$ -ethylene glycol appears similar to that in  $D_2O$ . The shift of the polyelectrolyte peak from  $Q_0=0.1 \text{ \AA}^{-1}$  to  $Q_0=0.077 \text{ \AA}^{-1}$  implies that in  $d$ -ethylene glycol, the interdistance between charged domains is larger than in  $D_2O$ . The spacing  $d_0 = 2\pi/Q_0 = 81.6 \text{ \AA}$  represents the average distance between charged domains, while the correlation length  $L$  corresponds to the average distance between neighboring entanglement points within the same domain. The high intensity of the SANS signal from poly(proline) is related to the presence of large size clusters and indicates that  $d$ -ethylene glycol is a poorer solvent than  $D_2O$  for poly(proline).

### Comparison between the temperature dependence of the scattering parameters in $D_2O$ and $d$ -ethylene glycol solutions

The scattering parameters obtained from the fits of Eq. 7 to the SANS spectra of poly(lysine) and poly(ethylene oxide) in the two solvents are compared in Fig. 9.  $D_2O$  and  $d$ -ethylene glycol exhibit opposite trends for the clustering intensity  $A/Q^n$ . Heating tends to increase clustering of poly(lysine) and poly(ethylene oxide) in  $D_2O$  and to decrease clustering of the same polymers in  $d$ -ethylene glycol. Figure 9 also shows that the LCST trend observed in  $D_2O$  is preserved when switching to  $d$ -ethylene glycol.

The trends observed for clustering and solvation intensity clearly indicate that these two phenomena are driven by different interactions: Clustering is primarily governed by hydrophobic effects, while solvation is mainly due to hydrophilic interactions.

### Conclusions

The present investigation is part of our concerted effort, using SANS, to determine solution structure and thermo-

dynamic properties of synthetic [19–22] as well as biological polymers [23–25].

SANS reveals that semi-dilute polymer solutions exhibit long-range clustering and short-range solvation properties. Clustering is due to hydrophobic groups sticking together to minimize contacts between polymer and solvent molecules. Solvation is driven by hydrophilic interactions (monomer–solvent attractive interactions) that keep the polymers hydrated (solvated) at the local level. Addition of salt to the solution of charged polymers shifts the polyelectrolyte peak towards lower values of  $Q$ , thus making the SANS spectra of polyelectrolyte solutions similar to that of neutral solutions.

We found that in aqueous solutions, both poly(ethylene oxide) and poly(lysine) separate upon heating. Ethylene glycol and water exhibit opposite trends for the clustering contribution, but identical trends for the solvation term.

Conventional research on biopolymers primarily focuses on the structure and function of complex biological molecules, such as proteins or DNA [26–28]. We are using SANS that probes structures over a wide range of length scales and provides insight into the hierarchical organization of the macromolecules as well as the phase behavior of the polymer system. This approach leads to understanding the physics of biopolymer solutions in simple terms, such as hydrophobic/hydrophilic interactions, clustering/solvation effects, mixed/separated phases, charged/neutral behaviors, etc. The present contribution is a modest step in that direction.

### Acknowledgments

**Disclaimer** Certain commercial equipment, instruments, or materials are identified in this paper to foster understanding. Such identification does not imply recommendation or endorsement by the National Institute of Standards and Technology, nor does it imply that the materials or equipment identified are necessarily the best available for the purpose. This work is based upon activities supported in part by the National Science Foundation under agreement no. DMR-0454672. F.H. acknowledges the support of the Intramural Research Program of the NICHD, NIH.

### References

1. Glatter O, Kratky O (1982) Small angle X-ray scattering. Academic, London
2. Jacrot B (1976) Study of biological structures by neutron-scattering from solution. Rep Prog Phys 39:911–953
3. Lovesey SW (1984) Theory of neutron scattering from condensed matter, vol. 1. Oxford University Press, Oxford
4. Higgins JS, Benoit HC (1994) Polymers and neutron scattering. Clarendon, Oxford
5. Schätzel K (1993) Dynamic light scattering. The method and some applications. Clarendon, Oxford
6. Ibel K, Stuhmann HB (1975) Comparison of neutron and X-ray-scattering of dilute myoglobin solutions. J Mol Biol 93:255–265

7. Engelman DM, Moore PB (1972) New method for determination of biological quaternary structure by neutron-scattering. *Proc Natl Acad Sci USA* 69:1997–1999
8. Svergun DI, Koch MHJ (2003) Small-angle scattering studies of biological macromolecules in solution. *Rep Prog Phys* 66:1735–1782
9. Feuz L, Strunz P, Geue T, Textor M, Borisov O (2007) Conformation of poly(L-lysine)-graft-poly(ethylene glycol) molecular brushes in aqueous solution studied by small-angle neutron scattering. *Eur Phys J E* 23:237–245
10. Flory PJ (1953) Principles of polymer chemistry. Cornell University Press, Ithaca
11. Sariban A, Binder K (1987) Critical properties of the Flory–Huggins lattice model of polymer mixtures. *J Chem Phys* 86:5859–5873
12. Stanley HE (1971) Introduction to phase transition and critical phenomena. Oxford University Press, New York
13. De Gennes PG (1979) Scaling concepts in polymer physics. Cornell University Press, Ithaca, New York
14. NIST Cold Neutron Research Facility, NG3 and NG7 30-m. SANS Instruments Data Acquisition Manual. January 2005
15. Edelman MW (2003) Segregative phase separation in aqueous mixtures of polydisperse biopolymers. PhD Thesis, University of Wageningen, The Netherlands
16. Prabhu VM, Muthukumar M, Wignall GW, Melnichenko YB (2003) Polyelectrolyte chain dimensions and concentration fluctuations near phase boundaries. *J Chem Phys* 119:4085–4098
17. Goldstein RE (1984) On the theory of lower critical solution points in hydrogen-bonded mixtures. *J Chem Phys* 80:5340–5341
18. Kjellander R, Florin E (1981) Water-structure and changes in thermal-stability of the system poly(ethylene oxide)-water. *J Chem Soc, Faraday Trans I* 77:2053–2077
19. Horkay F, Bassar PJ, Hecht AM, Geissler E (2000) Osmotic and SANS observations on sodium polyacrylate hydrogels in physiological salt solutions. *Macromolecules* 33:8329–8333
20. Horkay F, Hecht AM, Grillo I, Bassar PJ, Geissler E (2002) Experimental evidence for two thermodynamic length scales in neutralized polyacrylate gels. *J Chem Phys* 117:9103–9106
21. Hammouda B, Ho D, Kline SK (2004) Insight into solvation and clustering in PEO solutions. *Macromolecules* 37:6932–6937
22. Hammouda B, Horkay F, Becker M (2005) Clustering and solvation in poly(acrylic acid) polyelectrolyte solutions. *Macromolecules* 38:2019–2021
23. Whitten AE, Jacques DA, Hammouda B, Hanley T, King GF, Guss JM, Trehwella J, Langley DB (2007) The structure of the Sda–Kina complex suggests an allosteric mechanism of histidine kinase inhibition. *J Mol Biol* 368:407–420
24. Horkay F, Hecht AM, Geissler E (2006) Similarities between polyelectrolyte gels and biopolymer solutions. *J Polym Sci B, Polym Phys* 44:3679–3686
25. Horkay F, Hecht AM, Rochas C, Bassar PJ, Geissler E (2006) Anomalous small angle X-ray scattering determination of ion distribution around a polyelectrolyte biopolymer in salt solution. *J Chem Phys* 125:234904
26. Bloomfield VA (1996) DNA condensation. *Curr Opin Struct Biol* 6:334–341
27. Petrescu A, Receveur V, Calmettes P, Durand D, Desmadril M, Roux B, Smith JC (1997) Small-angle neutron scattering by a strongly denatured protein: analysis using random polymer theory. *Biophys J* 72:335–342
28. Bai Y, Das R, Millett IS, Herschlag D, Doniach S (2005) Probing counterion modulated repulsion and attraction between nucleic acid duplexes in solution. *Proc Natl Acad Sci USA* 102:1035–1040